

The Time-Marching Method of Fundamental Solutions for Multi-Dimensional Telegraph Equations

C.Y. Lin¹, M.H. Gu¹ and D.L. Young^{1,2}

Abstract: The telegraph equations are solved by using the meshless numerical method called the time-marching method of fundamental solutions (TMMFS) in this paper. The present method is based on the method of fundamental solutions, the method of particular solutions and the Houbolt finite difference scheme. The TMMFS is a meshless numerical method, and has the advantages of no mesh building and numerical quadrature. Therefore in this study we eventually solved the multi-dimensional telegraph equation problems in irregular domain. There are totally six numerical examples demonstrated, in order they are one-dimensional telegraph equation, one-dimensional non-decaying telegraph problem, two-dimensional telegraph equation in irregular domain, three-dimensional telegraph problem in cubic domain, three-dimensional telegraph equation in irregular domain and three-dimensional fixed boundary telegraph problem in irregular domain. All numerical results have shown good efficiency and accuracy of the algorithm, thus demonstrated the present meshless numerical method of the TMMFS is applicable for further applications in solving the multi-dimensional telegraph equation in irregular domain.

Keywords: Meshless numerical method, method of fundamental solutions, method of particular solutions, telegraph equation, damped wave equation

1 Introduction

The solution for the so-called multi-dimensional telegraph equation is approximated by applying meshless numerical method in this paper. The telegraph equation can be considered as a wave equation with damping and time-dependent loading terms, consists of the physical fields of vibration, propagation and diffusion, etc. The above physical characteristics of telegraph equations are usually used to

¹ Department of Civil Engineering and Hydrotech Research Institute, National Taiwan University, Taipei, Taiwan 10617

² Correspondence to: Prof. D.L. Young, E-mail: dlyoung@ntu.edu.tw, Tel and Fax: +886-2-2362-6114

explain the phenomena of electronic current propagation through a cable and with applications such as the telegraph signal transmission. Furthermore, the telegraph equation can also be applied to discuss the problems of wave, diffusion and conduction or the phenomena of molecular diffusion, conduction and radiation, etc.

Several means and ways have been applied to obtain the solutions of physical fields such as the theoretical analyses [Ortega and Robles-P'erez (1998)], experimental measurements and numerical simulations. Numerical simulation is a popular and powerful way to obtain the approximated solutions of partial differential equations. There were many mesh-dependent numerical methods such as finite difference methods (FDM) [Gao and Chi (2007)], finite element methods (FEM), finite volume methods (FVM), boundary element methods (BEM) [Sun, Huang, Liu and Cen (2004)] and spectral methods (SM), etc. They have been developed to approximate the solutions of partial differential equations. Although those above mentioned mesh-dependent numerical methods were largely adopted for science researches and engineering applications, some disadvantages also perplex the users such as the problems of mesh building, numerical quadrature and obtaining high accurate solutions, etc. These features however can be further improved by using the meshless or mesh free numerical schemes.

The meshless numerical methods include some advantages like avoiding mesh generation and numerical quadrature while having the good accuracy; therefore in order to reduce costs while obtaining good solution, we applied these meshless numerical methods to solve the multi-dimensional telegraph equations. There are many famous meshless numerical methods, such as the smoothed particle hydrodynamics (SPH) [Crespo, Gómez-Gesteira and Dalrymple (2007)], the multiquadric collocation method (MQCM) [Young, Chen and Wong, (2005); Amaziane, Naji and Ouazar (2004)], the method of fundamental solutions (MFS) [Young, Tsai, Lin and Chen (2006)], the meshless local Petrov-Galerkin method (MLPG) [Lin and Atluri (2001); Atluri, Han and Shen (2003); Han and Atluri (2003)] and the hyper-singular meshless method (HMM) [Young, Chen, Liu, Shen and Wu (2009)], etc. Among the meshless numerical methods, some have been applied to approximate the solutions of telegraph equations [Dehghan and Shokri (2007); Dehghan and Ghesmati (2010)].

The time-marching method of fundamental solutions is applied to deal with the telegraph problems in this study since it had shown good performance to solve the multi-dimensional wave problems [Young, Gu and Fan (2009)]. During 1960-1980, the method of fundamental solutions (MFS) was proposed and applied to approximate the solutions of the homogeneous elliptic-type partial differential equations [Kapradze and Aleksidze (1964); Mathon and Johnson (1977)]. The MFS was then combined with the method of particular solutions (MPS) for dealing with

the non-homogeneous elliptic problems [Golberg (1995)]. However, the two-stage MPS-MFS is difficult to solve the non-homogeneous elliptic-type equations with time-dependent source terms. Afterward, the MFS was applied by using diffusion fundamental solution to handle diffusion problems [Young, Tsai, Murugesan, Fan and Chen (2004)]. And the two-stage MPS-MFS was also used to solve the non-homogeneous diffusion problems [Young, Tsai and Fan (2004)]. However this method is still limited to the time-independent source terms. The Eulerian-Lagrangian method was then introduced to combine with the MFS (Eulerian-Lagrangian method of fundamental solutions, ELMFS) for approximating the solutions of partial differential equations such as the advection-diffusion equations [Young, Fan, Tsai, Chen and Murugedsan (2006)], Burgers' equation [Young, Fan, Hu and Atluri (2008)], advection equations and one-dimensional wave equations [Gu, Young and Fan (2009)]. Although the ELMFS is applicable for some simple wave problems, the ELMFS is still difficult to extend to treat the complex hyperbolic problems such as the multi-dimensional wave equations in irregular domain.

The applied TMMFS is a kind of meshless method which includes the characteristics of both the domain- and boundary-type meshless methods. The TMMFS was applied to analyze time-dependent partial differential equations [Cho, Golberg, Muleshkov and Li (2004)] and the conductive problems for functionally graded materials [Wang, Qin, and Kang (2006)]. The present meshless method considers the telegraph equation as a Poisson-type equation with time-dependent source terms. Through the time marching process the hyperbolic problems become the elliptic boundary value problems. The dual reciprocity boundary element method (DRBEM) is similar to the coupled MPS-MFS [Tsai, Young and Cheng (2002); Divo and Kassab (2005)], however the DRBEM is still time-consuming to construct the massive surface mesh and useful numerical quadrature.

The telegraph equation includes the second-order time-differentiation term and thus causing some computational problems for the MFS. The problems come from the Dirac delta function (or Heaviside function), which makes it difficult to obtain the numerical solution. The problem of time discretization can be solved by integral transforms [Davies, Crann, Kane and Lai (2007); Wen and Chen (2009); Liu (2010)], group-preserving scheme (GPS) [Liu, Chang, Chang and Chen (2008)], eigenfunction expansion method [Young, Chen, Fan and Shen (2009)] and the popular FDM which is adopted in this paper.

The telegraph equation can be considered as a Poisson equation with time-dependent source terms. The Houbolt FD scheme [Houbolt (1950); Soroushian and Farjoodi (2008)] is applied to discretize the transient terms of telegraph equation. After approximating the transient terms by the Houbolt FD scheme, the coupled MPS-MFS is applied for space discretization. In coupled MPS-MFS, the particular solution

and homogeneous solution satisfies the non-homogeneous equation and Laplace equation, respectively. In this study, the particular solution is approximated by radial basis functions while the homogeneous solution is dependent upon the Laplace fundamental solution.

There are six numerical experiments demonstrated in this paper. In order they are one-dimensional telegraph equation, one-dimensional non-decaying wave problem, two-dimensional telegraph equation in irregular domain, three-dimensional telegraph problem in cubic domain, three-dimensional telegraph equation in irregular domain and three-dimensional bounded telegraph problem in irregular domain. Solutions obtained by the TMMFS are compared with analytical solutions or solutions by the FEM, and all have shown good accuracy. The details of the applied TMMFS are explained in the following sections.

2 Governing Equation and Essential Conditions

The governing equation of the telegraph equation can be written as follows,

$$k_1 \frac{\partial^2 \varphi}{\partial t^2} + k_2 \frac{\partial \varphi}{\partial t} + k_3 \varphi = \nabla^2 \varphi + s(\vec{x}, t), \quad \vec{x} \in \Omega, \quad t > 0, \quad (1)$$

where $\varphi(\vec{x}, t)$ is the physical variable, $s(\vec{x}, t)$ is the source term, k_1, k_2 are positive constant coefficients, k_3 may take negative value, t denotes time and \vec{x} is the space vector, and Ω is the space domain.

We can show the variety of equations as in the above form, and it all can be solved by the time-marching MFS, such as the wave equation where $k_2 = k_3 = 0$; the damped wave equation where $k_3 = 0$; the diffusion equation where $k_1 = k_3 = 0$; and the Helmholtz equation where $k_1 = k_2 = 0, k_3 < 0$.

The initial conditions for the telegraph equation are listed as follows,

$$\varphi(\vec{x}, t)|_{t=0} = I_I(\vec{x}), \quad (2)$$

$$\left. \frac{\partial \varphi(\vec{x}, t)}{\partial t} \right|_{t=0} = I_{II}(\vec{x}), \quad (3)$$

where I_I is the first-kind initial condition, and I_{II} denotes the second-kind initial condition.

The boundary conditions are,

$$\varphi(\vec{x}, t)|_{\vec{x} \in \partial\Omega_1} = a_D(\vec{x}, t), \quad (4)$$

$$\left. \frac{\partial \varphi(\vec{x}, t)}{\partial \vec{n}} \right|_{\vec{x} \in \partial\Omega_2} = a_N(\vec{x}, t), \quad (5)$$

where $\partial\Omega = \partial\Omega_1 \cup \partial\Omega_2$ is the boundary of the domain, \vec{n} is an outward unit normal vector of boundary, a_D and a_N denote functions of time and space, and subscripts D and N denote the Dirichlet-type and Neumann-type boundary conditions, respectively.

3 Numerical Method

The governing equation can be considered as a Poisson-type equation with time-dependent loading and source term after discretizing the time domain. In order to avoid the difficult problems of constructing the linear system by initial conditions, the time-integration scheme is needed for discretizing the time domain, therefore the Houbolt FD scheme is selected for the time discretization. The so-called Houbolt FD model is an unconditionally stable and high accuracy time-integration scheme, the first- and second-order time-differentiation terms are listed as follows,

$$\frac{\partial\varphi^{n+1}}{\partial t} \approx \frac{1}{6\Delta t}(11\varphi^{n+1} - 18\varphi^n + 9\varphi^{n-1} - 2\varphi^{n-2}), \quad (6)$$

$$\frac{\partial^2\varphi^{n+1}}{\partial t^2} \approx \frac{1}{\Delta t^2}(2\varphi^{n+1} - 5\varphi^n + 4\varphi^{n-1} - \varphi^{n-2}), \quad (7)$$

where $\varphi^n = \varphi(\vec{x}, t^n)$, $t^n = n\Delta t$, Δt is the time interval, and n denotes the time level. Since the governing equation can be transferred into a Poisson-type equation with time-dependent source terms by using the Houbolt FD method for the time operators, we can write:

$$\nabla^2\varphi^{n+1} = C_0\varphi^{n+1} + C_1\varphi^n + C_2\varphi^{n-1} + C_3\varphi^{n-2} - s^{n+1}(\vec{x}, t), \quad (8)$$

$$C_0 = \frac{2k_1}{\Delta t^2} + \frac{11k_2}{6\Delta t} + k_3, \quad C_1 = -\frac{5k_1}{\Delta t^2} - \frac{3k_2}{\Delta t}, \quad C_2 = \frac{4k_1}{\Delta t^2} + \frac{3k_2}{2\Delta t}, \quad C_3 = -\frac{k_1}{\Delta t^2} - \frac{k_2}{3\Delta t}.$$

In the coupled MPS-MFS, the solution for physical variable can be defined as:

$$\varphi^{n+1} = \varphi_H^{n+1} + \varphi_P^{n+1}, \quad (9)$$

where φ_H is the homogeneous solution which satisfies the Laplace equation and φ_P is the particular solution which satisfies the non-homogeneous equation.

The homogeneous solution φ_H can be approximated by the linear combination of fundamental solutions as follows,

$$\varphi_H^{n+1} = \sum_{j=1}^{N_B} \alpha_j^{n+1} G(\|\vec{x} - \vec{\xi}_j\|), \quad (10)$$

where $G()$ is the fundamental solution, α_j is the intensity of source points, N_B is the number of boundary points, \vec{x} is the space location of field points, $\vec{\xi}$ is the space location of source points, and the subscript j denotes the index of the source points.

The fundamental solutions of the Laplace equation are listed as follows,

$$G(\|\vec{x} - \vec{\xi}\|) = \begin{cases} \frac{-1}{2} \|\vec{x} - \vec{\xi}\|, & \text{for 1 - D} \\ \frac{-1}{2\pi} \ln(\|\vec{x} - \vec{\xi}\|), & \text{for 2 - D} \\ \frac{1}{4\pi \|\vec{x} - \vec{\xi}\|^2}, & \text{for 3 - D} \end{cases} \quad (11)$$

In this paper, the particular solution φ_P is approximated by the linear combination of the radial basis functions (RBF) as:

$$\varphi_P^{n+1} = \sum_{j=1}^N \beta_j^{n+1} F(r_j). \quad (12)$$

The $F()$ can be obtained from integration of the Laplacian as in the following,

$$\nabla^2 F(r) = f(r), \quad (13)$$

where $f()$ is the radial basis function, $F()$ is the integrated radial basis function, β_j is the coefficient vector of basis function, N is the number of field points, and the subscript j denotes the index of collocation points.

The compactly supported radial basis functions (CSRBF) [Chen, Brebbia and Power (1999)] is chosen to describe the particular solution in multi-dimensional space.

The $f(r)$ and $F(r)$ described by CSRBF can be written as

$$f(r) = \begin{cases} (1 - \frac{r}{\lambda})^2, & r \leq \lambda \\ 0, & r > \lambda \end{cases} \quad (14)$$

$$F(r) = \begin{cases} \frac{r^4}{12\lambda^2} - \frac{r^3}{3\lambda} + \frac{r^2}{2}, & r \leq \lambda, \text{ for 1 - D} \\ \frac{\lambda^2}{4} + \frac{\lambda}{3} (r - \lambda), & r > \lambda, \text{ for 1 - D} \\ \frac{r^4}{16\lambda^2} - \frac{2r^3}{9\lambda} + \frac{r^2}{4}, & r \leq \lambda, \text{ for 2 - D} \\ \frac{13\lambda^2}{144} + \frac{\lambda^2}{12} \ln\left(\frac{r}{\lambda}\right), & r > \lambda, \text{ for 2 - D} \\ \frac{r^4}{20\lambda^2} - \frac{r^3}{6\lambda} + \frac{r^2}{6}, & r \leq \lambda, \text{ for 3 - D} \\ \frac{\lambda^2}{12} - \frac{\lambda^3}{30r}, & r > \lambda, \text{ for 3 - D} \end{cases} \quad (15)$$

where r is the distance between the field points and the λ is the compact radius of the CSRBF.

According to the definitions of particular and homogeneous solutions, the governing equation can be rewritten as:

$$\nabla^2 \varphi_P^{n+1} = C_0(\varphi_P^{n+1} + \varphi_H^{n+1}) + C_1 \varphi^n + C_2 \varphi^{n-1} + C_3 \varphi^{n-2} - s^{n+1}(\vec{x}, t). \quad (16)$$

After substituting Eq. (10) and Eq. (12) into Eq. (16), we can obtain:

$$\begin{aligned} \sum_{j=1}^N \beta_j^{n+1} (f(r_j) - C_0 F(r_j)) - \sum_{j=1}^{N_B} \alpha_j^{n+1} C_0 G(\|\vec{x} - \vec{\xi}_j\|) \\ = C_1 \varphi^n + C_2 \varphi^{n-1} + C_3 \varphi^{n-2} - s^{n+1}(\vec{x}, t) \end{aligned} \quad (17)$$

The boundary conditions can be expressed as:

$$B(\varphi) = b(\vec{x}, t), \quad \vec{x} \in \partial\Omega, \quad (18)$$

where $B()$ denotes the boundary operator and b denotes the function which is described by boundary conditions. The boundary conditions can be rewritten as follows,

$$\left[\sum_{j=1}^N \beta_j^{n+1} B(F(r_j)) + \sum_{j=1}^{N_B} \alpha_j^{n+1} B\left(G(\|\vec{x} - \vec{\xi}_j\|)\right) \right] \Big|_{\vec{x} \in \partial\Omega} = b(\vec{x}, t^{n+1}). \quad (19)$$

The linear system can be expressed as:

$$\begin{bmatrix} A_1 & A_2 \\ A_3 & A_4 \end{bmatrix} \begin{Bmatrix} \beta^{n+1} \\ \alpha^{n+1} \end{Bmatrix} = \begin{Bmatrix} S \\ b \end{Bmatrix},$$

where the sub-elements in the linear system are

$$A_1 = f(r) - C_0 F(r), \quad A_2 = -C_0 G(\|\vec{x} - \vec{\xi}\|), \quad A_3 = B(F(r)), \quad A_4 = B\left(G(\|\vec{x} - \vec{\xi}\|)\right), \quad (20)$$

$$S = C_1 \varphi^n + C_2 \varphi^{n-1} + C_3 \varphi^{n-2} - s^{n+1}(\vec{x}, t).$$

In order to avoid the setup problem of time stepping, the Euler scheme is used to obtain the subcomponents φ^{n-1} and φ^{n-2} into the vector S as

$$\begin{cases} \varphi^{n-1} = I_I(\vec{x}) - \Delta t \cdot I_{II}(\vec{x}) \\ \varphi^{n-2} = I_I(\vec{x}) - 2\Delta t \cdot I_{II}(\vec{x}) \end{cases}, \quad n \leq 2, \quad (21)$$

The vectors α and β can be obtained by the linear system solver, then the solution in the computational domain can be calculated from the definition of particular and homogeneous solutions as follows.

$$\varphi^{n+1} = \sum_{j=1}^N \beta_j^{n+1} F(r_j) + \sum_{j=1}^{N_B} \alpha_j^{n+1} G(\|\vec{x} - \vec{\xi}_j\|). \quad (22)$$

4 Numerical Examples

The applied model for solving the telegraph equation problems is tested by considering the following six numerical experiments. In order to make sure the capability of the proposed meshless telegraph model, numerical solutions are compared with analytical solutions or solutions by the FEM.

In this paper, the maximum relative error and the L^2 norm error are defined as follows,

$$E_{Rel} = \frac{Max(|\varphi_{i,Analytical} - \varphi_{i,Numerical}|)}{Max(|\varphi_{i,Analytical}|)}, \quad (23a)$$

$$E_{L^2} = \left(\frac{\sum_{i=1}^M (\varphi_{i,Analytical} - \varphi_{i,Numerical})^2}{\sum_{i=1}^M \varphi_{i,Analytical}^2} \right)^{\frac{1}{2}}, \quad (23b)$$

where M is the number of resolution points.

4.1 Example 1: 1-D telegraph equation

For this example, a one-dimensional telegraph equation is considered to validate the capability of the applied scheme. The physical field is governed by the equation of

$$\frac{\partial^2 \varphi}{\partial t^2} + 8 \frac{\partial \varphi}{\partial t} + 4\varphi = \frac{\partial^2 \varphi}{\partial x^2} + s(x,t), \quad t > 0, \quad x \in (0,5), \quad t > 0, \quad (24)$$

where $s(x,t) = -2e^{-t} \sin x + 4$.

The initial displacement and velocity are:

$$\varphi(x,t)|_{t=0} = \sin x + 1 \quad \text{and} \quad \left. \frac{\partial \varphi(x,t)}{\partial t} \right|_{t=0} = -\sin x. \quad (25)$$

While boundary conditions are given as:

$$\varphi(x,t)|_{x=0} = 1 \quad \text{and} \quad \varphi(x,t)|_{x=5} = e^{-t} \sin 5 + 1, \quad t > 0. \quad (26)$$

The analytical solution of this problem is:

$$\varphi(x,t) = e^{-t} \sin x + 1 \quad (27)$$

The uniform point distribution is selected for this numerical case. Figure 1 shows the solution obtained by the applied method at different time, where numerical

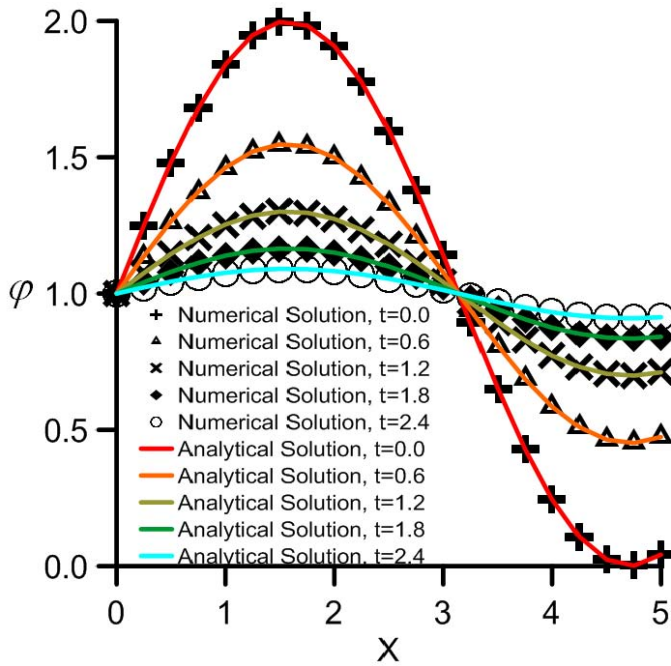


Figure 1: The evolution of displacement for example 1 by using 21 points, $\Delta t = 0.001$.

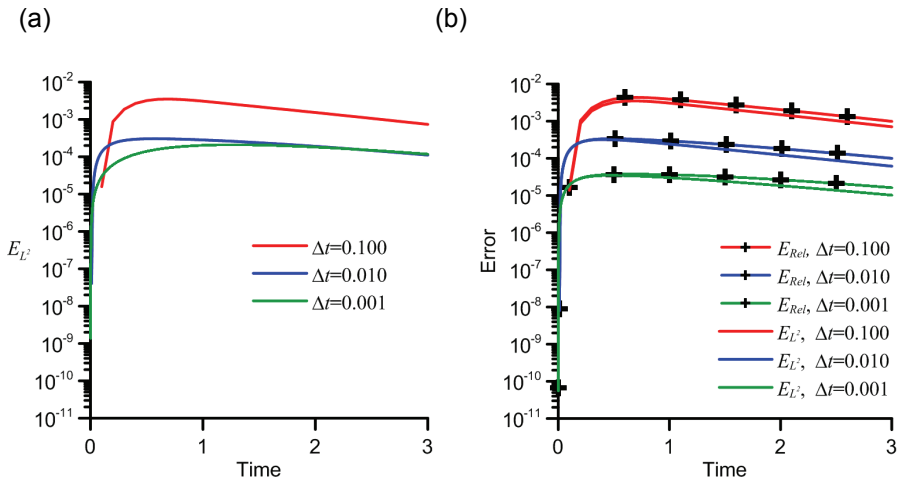


Figure 2: The error distribution by the TMMFS for example 1 using (a) 21 points (b) 101 points.

solutions are well matched with analytical solutions. The error distributions of E_{Rel} and E_{L^2} dependent on different Δt are shown in Figs. 2 (a) and (b) by using 21 and 101 points, respectively. It can be observed that as time interval decreases, all error decreases as well. Also the dependence of error distribution with time is observed, error decays as time elapses. Hereby we have validated the applied method is capable for solving one-dimensional telegraph equation.

4.2 Example 2: 1-D non-decaying telegraph problem

In the second example, the one-dimensional non-decaying telegraph problem is considered to demonstrate the capability of the present method for dealing with the non-decaying phenomena. The physical field is governed by the equation as:

$$\frac{\partial^2 \varphi}{\partial t^2} + 12 \frac{\partial \varphi}{\partial t} + 4\varphi = \frac{\partial^2 \varphi}{\partial x^2} + s(x,t), \quad t > 0, \quad x \in (0,6), \quad (28)$$

where $s(x,t) = -12 \sin t \sin x + 4 \cos t \sin x + 8$.

The initial displacement and the velocity are listed as follows,

$$\varphi(x,t)|_{t=0} = 2 + \sin x \quad \text{and} \quad \left. \frac{\partial \varphi(x,t)}{\partial t} \right|_{t=0} = 0. \quad (29)$$

While boundary conditions are given as:

$$\varphi(x,t)|_{x=0} = 2 \quad \text{and} \quad \varphi(x,t)|_{x=6} = 2 + \cos t \sin 6, \quad t > 0. \quad (30)$$

The analytical solution of this problem is written as:

$$\varphi(x,t) = 2 + \cos t \sin x. \quad (31)$$

The uniform point distribution is used for testing the proposed meshless method. Figure 3 displays the evolution of physical field with different time. We can observe that the numerical solutions obtained by applying the TMMFS are compared well with the analytical solutions. The period of the physical field is π in this case, Fig. 4 displays the error distributions of E_{Rel} and E_{L^2} with more than 60 cycles of oscillation.

In this case, the physical field does not decay as time increases. If the pattern of E_{Rel} and E_{L^2} of the TMMFS stays in the same order and does not increase as time increases, the applied method can be considered with good performances. Figure 4 has shown the dependence of error distribution on different time interval Δt , and error distributions maintain the same order as time elapses. The error distribution explains the TMMFS is a stable and accurate numerical method.

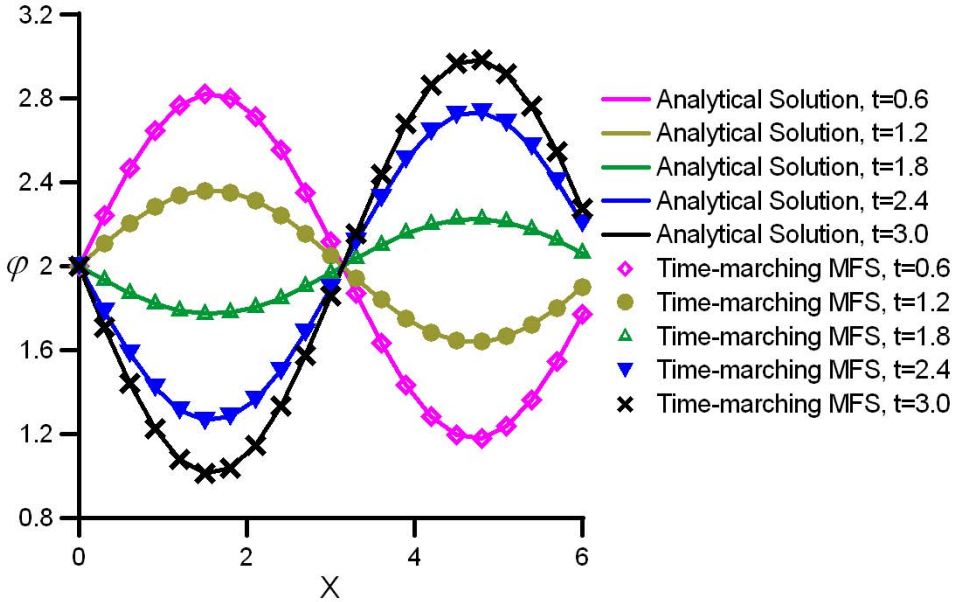


Figure 3: The evolution of displacement φ for example 2 by using 21 points, $\Delta t = 0.001$.

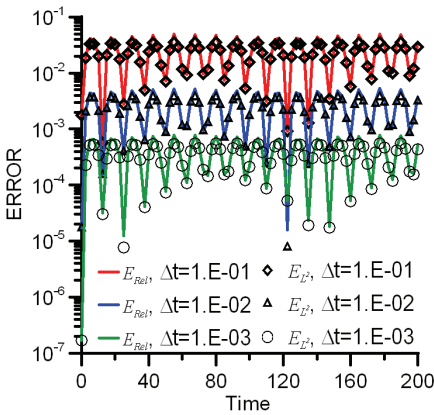


Figure 4: The error distribution by the TMMFS using 21 field points, error evaluated every 25, 250, 2500 points for $\Delta t = 0.1, 0.01, 0.001$.

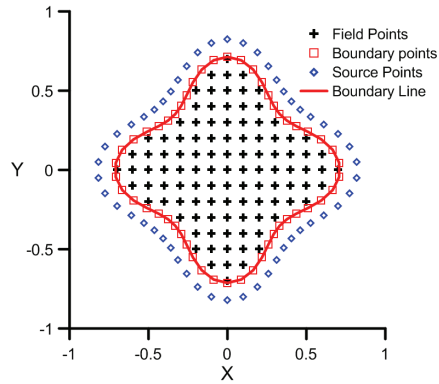


Figure 5: The point distribution of the two-dimensional problem in example 3.

4.3 Example 3: 2-D telegraph equation in irregular domain

This example is a two-dimensional telegraph equation in irregular domain with smooth edge. It is considered to demonstrate the capability of the TMMFS for 2-D

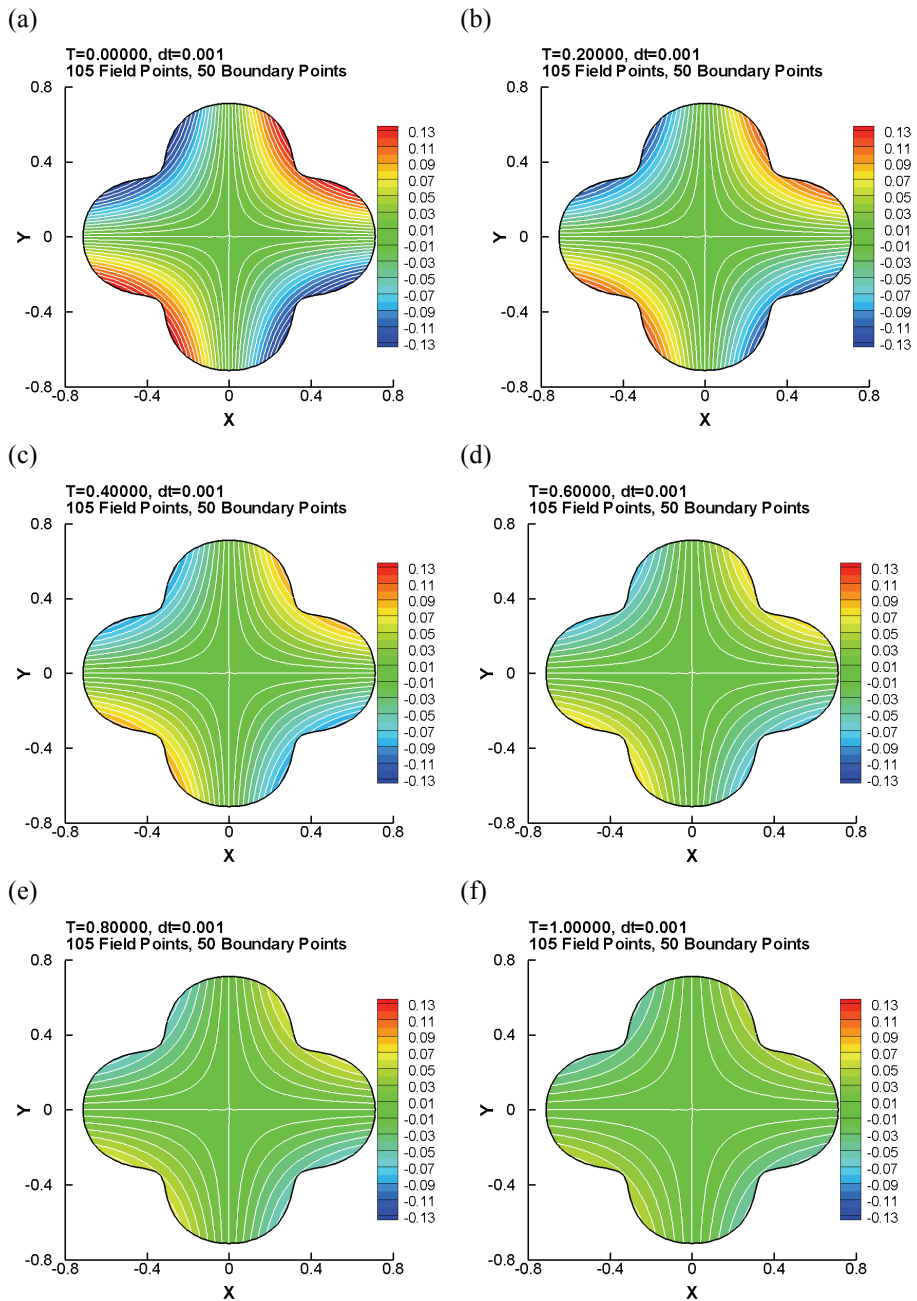


Figure 6: The evolution of displacement for example 3, at (a) $t = 0.0$ (b) $t = 0.2$ (c) $t = 0.4$ (d) $t = 0.6$ (e) $t = 0.8$ (f) $t = 1.0$.

telegraph equation in irregular domain. The space domain Ω and its boundary $\partial\Omega$ are defined by the following curve:

$$\partial\Omega = \left\{ (x,y) \mid \begin{array}{l} x = R_C \cos \theta, \\ y = R_C \sin \theta, \end{array} \quad 0 < \theta \leq 2\pi \right\}, \quad (32)$$

where R_C is defined as:

$$R_C = \frac{1}{2} \left(\cos 4\theta + \sqrt{\frac{18}{5} - \sin^2 \theta} \right)^{1/3}. \quad (33)$$

In this example, the governing equation is set as:

$$\frac{\partial^2 \varphi}{\partial t^2} + 2 \frac{\partial \varphi}{\partial t} + \varphi = \nabla^2 \varphi + s(x,y,t), \quad t > 0, \quad (x,y) \in \Omega, \quad (34)$$

where $s(x,y,t) = 2e^{-t} \sin x \sin y$.

The initial displacement and the velocity are:

$$\varphi(x,y,t)|_{t=0} = \sin x \sin y \quad \text{and} \quad \left. \frac{\partial \varphi(x,y,t)}{\partial t} \right|_{t=0} = -\sin x \sin y. \quad (35)$$

While boundary conditions are

$$\varphi(x,y,t)|_{(x,y) \in \partial\Omega} = e^{-t} \sin x \sin y, \quad t > 0. \quad (36)$$

The analytical solution for this problem is listed as follows,

$$\varphi(x,y,t) = e^{-t} \sin x \sin y. \quad (37)$$

We used 105 field points and 50 boundary points for the TMMFS collocation. The points are uniformly distributed in the domain as shown in Fig. 5. Figure 6 depicts the evolution of the displacement with different time. It is revealed that the physical value φ forms a saddle shape with the saddle point at the origin and the magnitude decreases as time increases.

Figure 7 (a) and (b) shows the error distributions by different time interval, as the time interval decreases the accuracy increases. From error distributions we can observe that E_{Rel} shows similar pattern comparing with E_{L^2} , both errors remain stable and oscillate in the same order. It means that the applied method has a good accuracy for both time and space.

In order to further discuss the accuracy of the applied method, the FEM is used to combine with the Houbolt scheme for solving the same problem by using 625

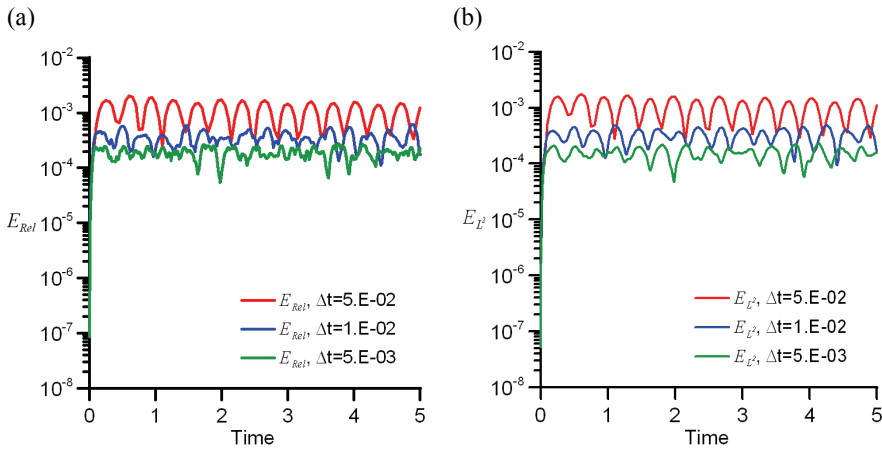


Figure 7: The error distributions of a) E_{Rel} b) E_{L^2} TMMFS for example 3 by using 105 field points and 50 boundary points, each error maintains in the same order.

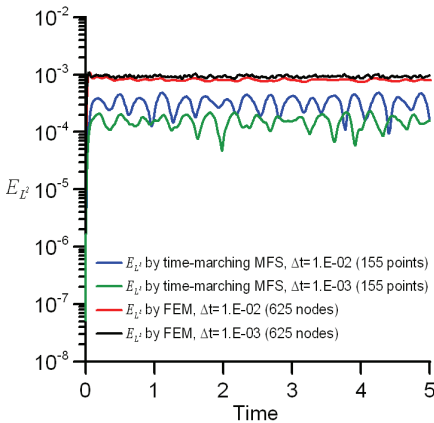


Figure 8: The E_{L^2} distribution by the TMMFS and FEM for example 3.

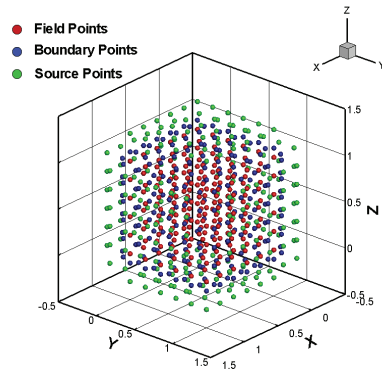


Figure 9: The point distribution of the cubic domain in example 4.

nodes (linear unstructured triangle element) under different time intervals. Figure 8 displays the history evolutions of E_{L^2} by the FEM and the applied method with different time interval. We can observe that the time interval effect for the FEM is not sensitive, although more nodes have been used. Therefore we indirectly prove the advantage of the applied method by using lower nodes to obtain a reasonable solution.

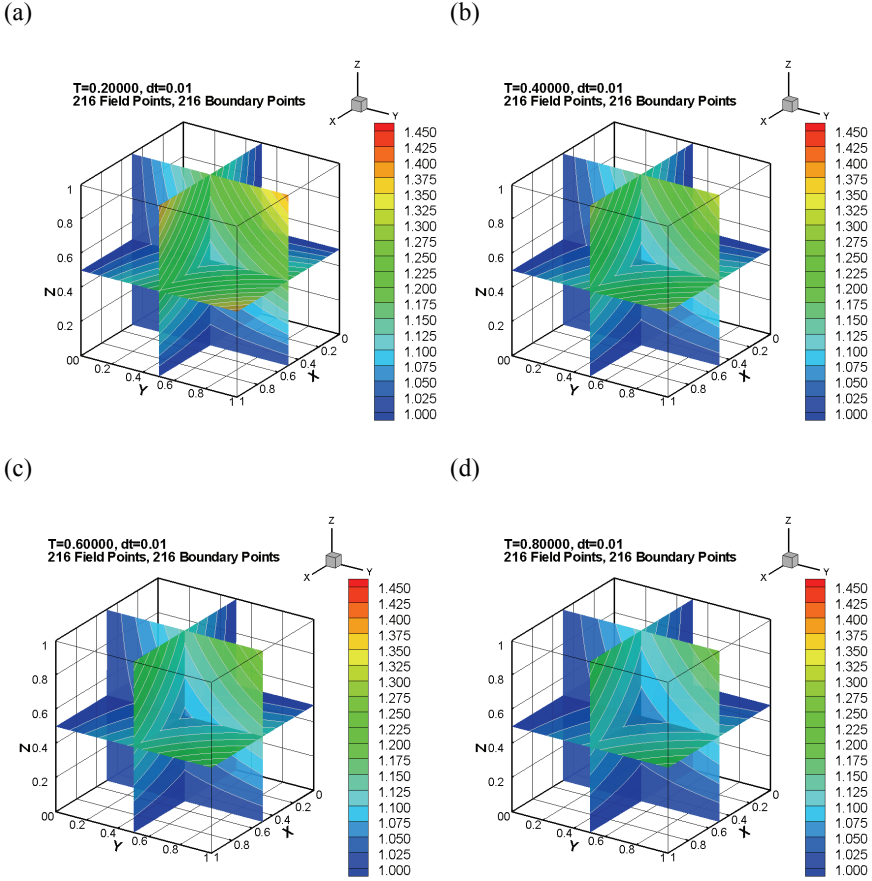


Figure 10: The evolution of φ for example 4 at profiles $x = 0.5, y = 0.5$ and $z = 0.5$, at (a) $t = 0.2$ (b) $t = 0.4$ (c) $t = 0.6$ (d) $t = 0.8$.

4.4 Example 4: The 3-D telegraph problem in cubic domain

In this example, the three-dimensional telegraph problem is considered in a cubic domain for demonstrating the capability of the applied method.

In this case, the governing equation is set as:

$$\frac{\partial^2 \varphi}{\partial t^2} + \frac{\partial \varphi}{\partial t} + \varphi = \nabla^2 \varphi + s(x, y, z, t), \quad t > 0, \quad (x, y, z) \in \Omega, \tag{38}$$

where $s(x, y, z, t) = e^{-t}(\sin xyz)(x^2y^2 + y^2z^2 + x^2z^2 + 1) + 1$.

The initial conditions are:

$$\varphi(x, y, z, t)|_{t=0} = 1 + \sin xyz \text{ and } \left. \frac{\partial \varphi(x, y, z, t)}{\partial t} \right|_{t=0} = -\sin xyz. \quad (39)$$

While boundary conditions are given as:

$$\varphi(x, y, z, t)|_{(x,y,z) \in \partial\Omega} = 1 + e^{-t} \sin xyz, \quad t > 0. \quad (40)$$

This problem has the analytical solution of

$$\varphi(x, y, z, t) = 1 + e^{-t} \sin xyz. \quad (41)$$

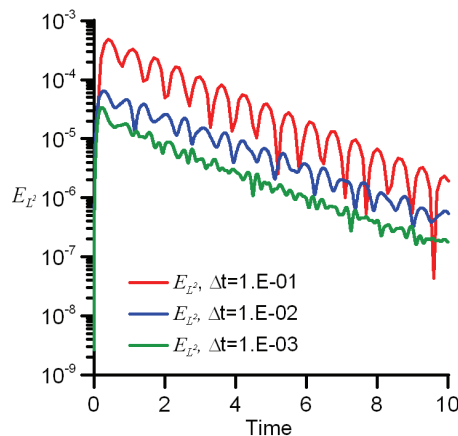


Figure 11: The E_{L^2} distribution by the TMMFS for example 4 by using 216 field points and 216 boundary points.

The uniform point distribution is used in this case to implement the calculation works of 216 field points and 216 boundary points as shown in Fig. 9. Figure 10 (a)-(d) shows field profile changes with time at $x = 0.5$, $y = 0.5$ and $z = 0.5$, respectively.

Figure 11 is the error distribution of E_{L^2} based on different time interval; it can be observed that when the time interval decreases, error distribution also decreases. In this case we have validated the applied method is suitable for dealing with three-dimensional telegraph problems.

4.5 Example 5: 3-D telegraph equation in irregular domain

This example is the three-dimensional telegraph equation in an irregular domain with smooth edge. The computational domain Ω and boundary $\partial\Omega$ are defined as follows,

$$\partial\Omega = \left\{ (x, y, z) \mid \begin{array}{l} x = R_C \sin \psi \cos \theta, \\ y = R_C \sin \psi \sin \theta, \\ z = R_C \cos \psi, \end{array} \quad 0 < \psi \leq \pi, \quad 0 < \theta \leq 2\pi \right\}, \quad (42)$$

where R_C is defined as:

$$R_C = 3 \left[\cos 3\theta + \sqrt{8 - \sin^2 3\theta} \right]^{1/3}. \quad (43)$$

In this example, the governing equation is set as:

$$4 \frac{\partial^2 \varphi}{\partial t^2} + \frac{\partial \varphi}{\partial t} + 2\varphi = \nabla^2 \varphi + s(x, y, z, t), \quad t > 0, \quad (x, y, z) \in \Omega, \quad (44)$$

where $s(x, y, z, t) = \left[\sin t + \left(\frac{3\pi^2}{16} - 2 \right) \cos t \right] e^{-\frac{t}{4}} \cos \frac{\pi x}{4} \cos \frac{\pi y}{4} \cos \frac{\pi z}{4} + 10$.

The initial conditions are listed as follows,

$$\varphi(x, y, z, t)|_{t=0} = 5 + \cos \frac{\pi x}{4} \cos \frac{\pi y}{4} \cos \frac{\pi z}{4} \quad (45)$$

and

$$\frac{\partial \varphi(x, y, z, t)}{\partial t} \Big|_{t=0} = -\frac{1}{4} \cos \frac{\pi x}{4} \cos \frac{\pi y}{4} \cos \frac{\pi z}{4}.$$

While boundary conditions are given as:

$$\varphi(x, y, z, t)|_{(x, y, z) \in \partial\Omega} = 5 + e^{-\frac{t}{4}} \cos t \cos \frac{\pi x}{4} \cos \frac{\pi y}{4} \cos \frac{\pi z}{4}, \quad t > 0. \quad (46)$$

The analytical solution for this example can be given as:

$$\varphi(x, y, z, t) = 5 + e^{-\frac{t}{4}} \cos t \cos \frac{\pi x}{4} \cos \frac{\pi y}{4} \cos \frac{\pi z}{4}. \quad (47)$$

Here we still use uniform point distribution for collocating 888 field points and 222 boundary points as depicted in Fig. 12. Figure 13 (a)-(d) shows the physical field profiles with different time at $x = 0$, $y = 0$ and $z = 0$, respectively by using 888 field points and 222 boundary points. The figures depict that the physical value φ

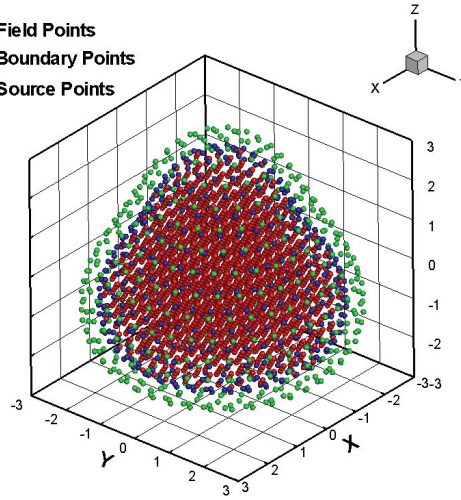


Figure 12: The point distribution of the three-dimensional problem in irregular domain in example 5 and 6.

decays and vibrates as time increases. From Fig. 13 (a)-(d), we can also discover that the physical field has vibrated one cycle at $t = 2\pi$ while the field value had been diffused.

Figure 14(a)-(c) indicates that when the time interval decreases, the errors decrease. Error distributions decay as time increases, and oscillate with a period of $t = 2n\pi$, and the patterns are all similar, showing the result is very reasonable.

Finally we compare the results by the proposed TMMFS model and the FEM model (with 16,003 and 39,318 nodes). In Fig. 15, it is clearly detected that the applied TMMFS telegraph model is not only more efficient, but also more accurate than the FEM in this case, therefore the applied method is a highly efficient meshless numerical method for dealing with the 3-D telegraph equation even with irregular domain.

4.6 Example 6: 3-D fixed boundary telegraph problem in irregular domain

The last test example is the three-dimensional bounded telegraph problem in irregular domain with smooth edge. The computational domain Ω and boundary $\partial\Omega$ are the same as example 5.

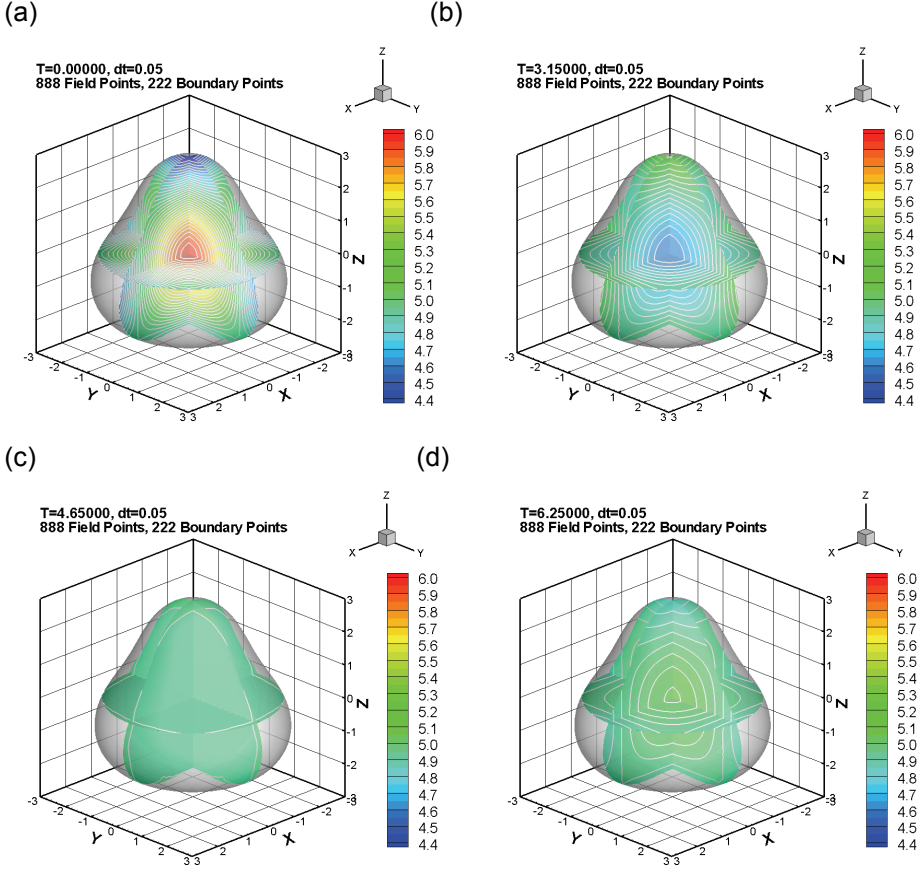


Figure 13: The evolution of φ for example 5 in slices at $x = 0, y = 0$ and $z = 0$, at (a) $t = 0.00$ (b) $t = 3.15$ (c) $t = 4.65$ (d) $t = 6.25$.

In this example, the governing equation is set as:

$$\frac{\partial^2 \varphi}{\partial t^2} + \frac{1}{4} \frac{\partial \varphi}{\partial t} = \nabla^2 \varphi, \quad t > 0, \quad (x, y, z) \in \Omega, \quad (48)$$

The initial condition are listed as follows,

$$\varphi(x, y, z, t)|_{t=0} = 5 \cos\left(\frac{3\pi\vec{x}}{2R_C}\right) \quad \text{and} \quad \frac{\partial \varphi(x, y, z, t)}{\partial t} \Big|_{t=0} = 0 \quad (49)$$

While boundary conditions are given as:

$$\varphi(x, y, z, t)|_{(x,y,z) \in \partial\Omega} = 0, \quad t > 0. \quad (50)$$

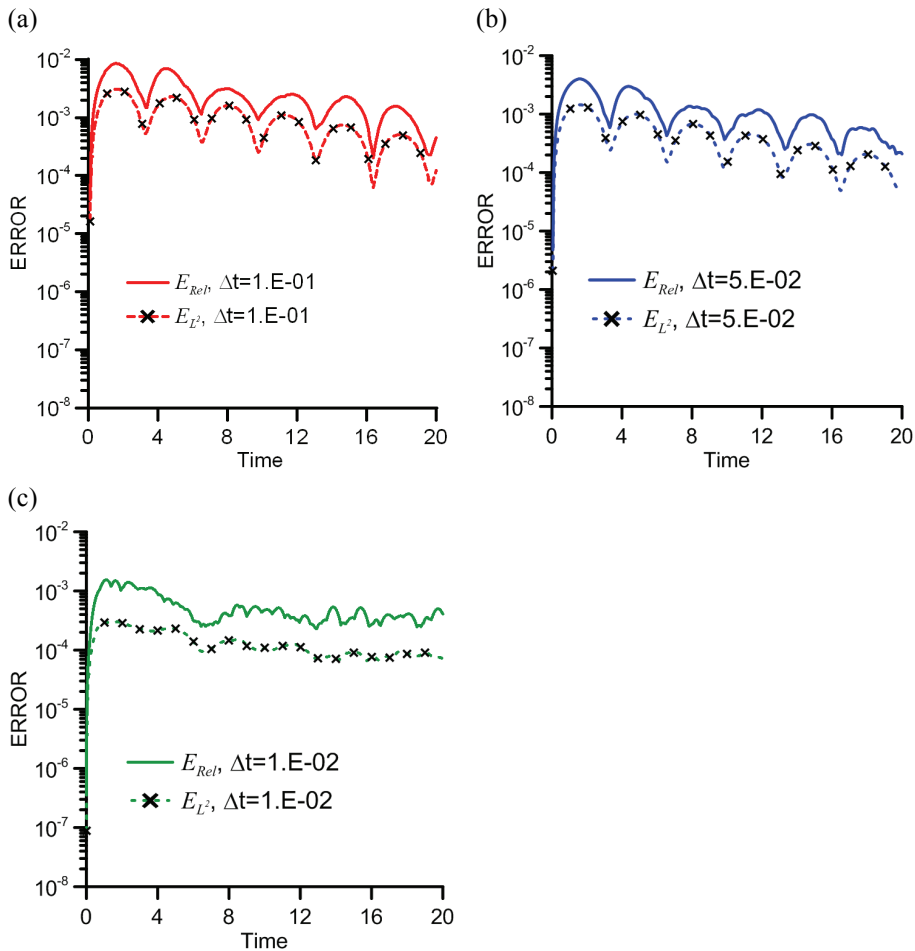


Figure 14: The error distribution by the TMMFS for example 5 using 888 field points and 222 boundary points (a) $\Delta t = 0.1$ (b) $\Delta t = 0.05$ (c) $\Delta t = 0.01$.

The uniform point distribution is still used in this case, field points and boundary points are the same as example 5 (Fig. 12). Figure 16 (a)-(f) shows field profile changes with time at $x = 0$, $y = 0$ and $z = 0$, respectively.

Since no analytical solution is available in this case, the solution of the TMMFS is compared with the solution of the FEM. In Fig. 17 (a)-(d) we show the distribution of the solution of the TMMFS and the solution of the FEM, and we can see both solutions are very close each other at the chosen points. Since similar solutions are obtained from both methods, we have shown the present method is capable to

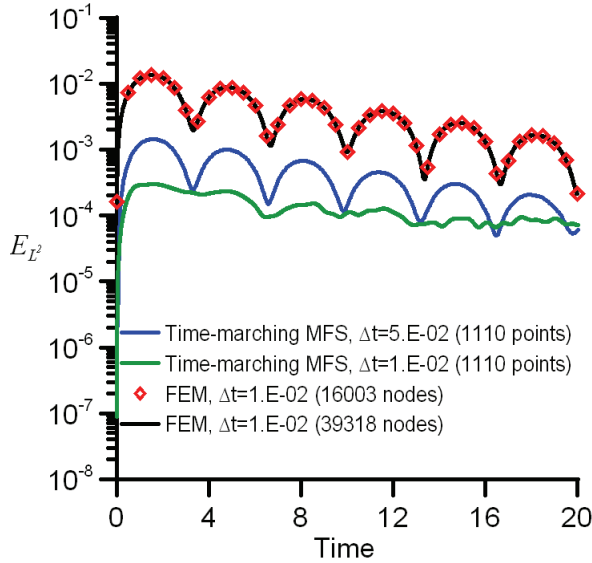


Figure 15: For example 5, the E_{L^2} of the TMMFS and FEM compared with analytical solutions.

obtain similar solution as mesh-dependent numerical methods for fixed boundary problems.

5 Conclusion

The problems of multi-dimensional telegraph equations in regular or irregular domain have been solved with sufficient efficiency and accuracy by the proposed TMMFS model. The TMMFS is a meshless method; it needs neither mesh generator nor any numerical quadrature. It is based on the Houbolt FD scheme to discretize time domain and the coupled MPS-MFS is applied to deal with the partial differential equations in the form of Poisson-type equations. All six numerical experiments, namely, one-dimensional telegraph equation, one-dimensional non-decaying wave problem, two-dimensional telegraph equation in irregular domain, three-dimensional telegraph problem in cubic domain, three-dimensional telegraph equation in irregular domain and three-dimensional fixed boundary telegraph problem in irregular domain, have been analyzed. When compared with analytical solutions, all cases have shown high accuracy and good stability. The third case and the fifth case have been compared with solutions obtained from the FEM, both showing the present method not only costs less, but also is more accurate. The sixth case has been compared with the solution of the FEM, showing the present method is ca-

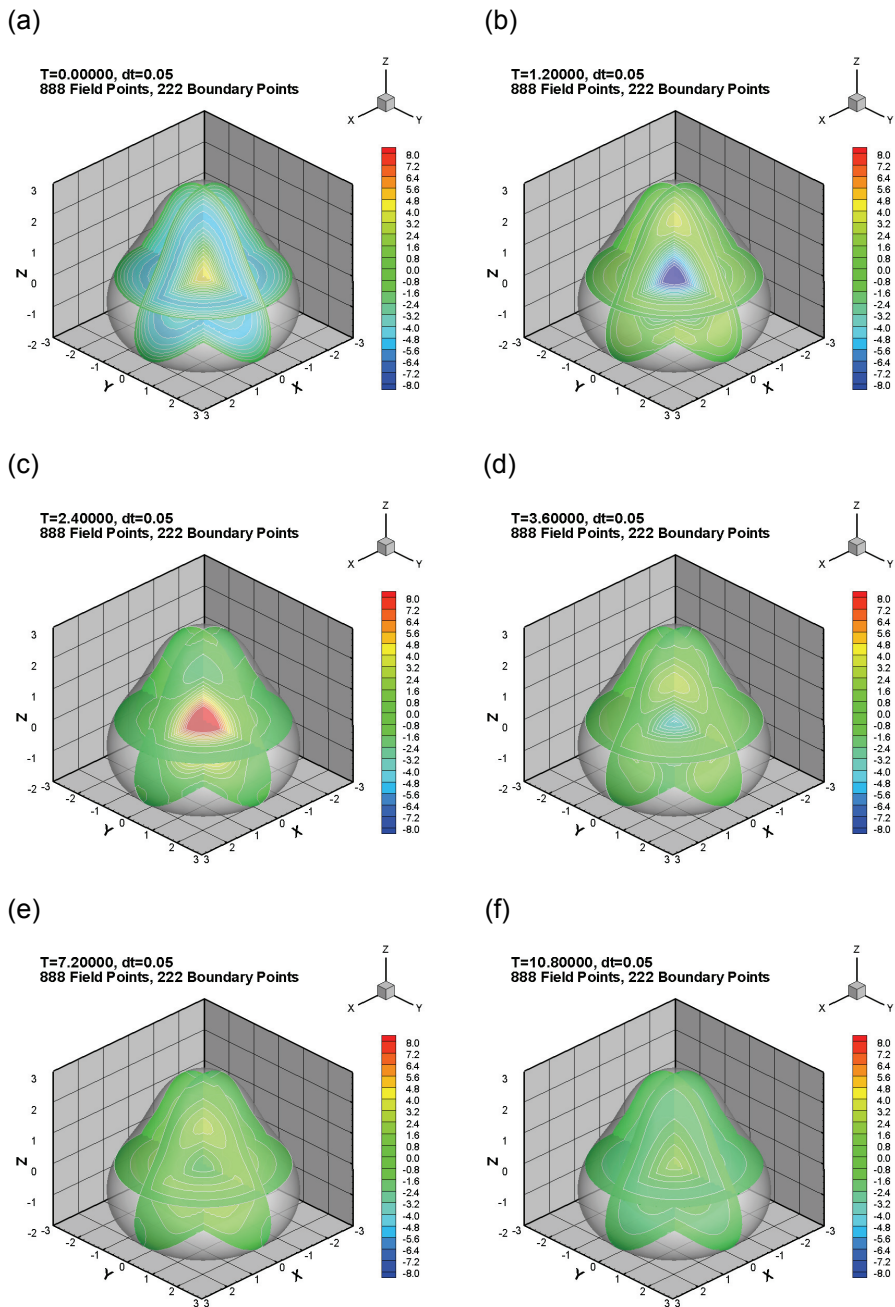


Figure 16: The evolution of φ for example 6 in slices at $x = 0, y = 0$ and $z = 0$, at (a) $t = 0.0$ (b) $t = 1.2$ (c) $t = 2.4$ (d) $t = 3.6$ (e) $t = 7.2$ (f) $t = 10.8$.

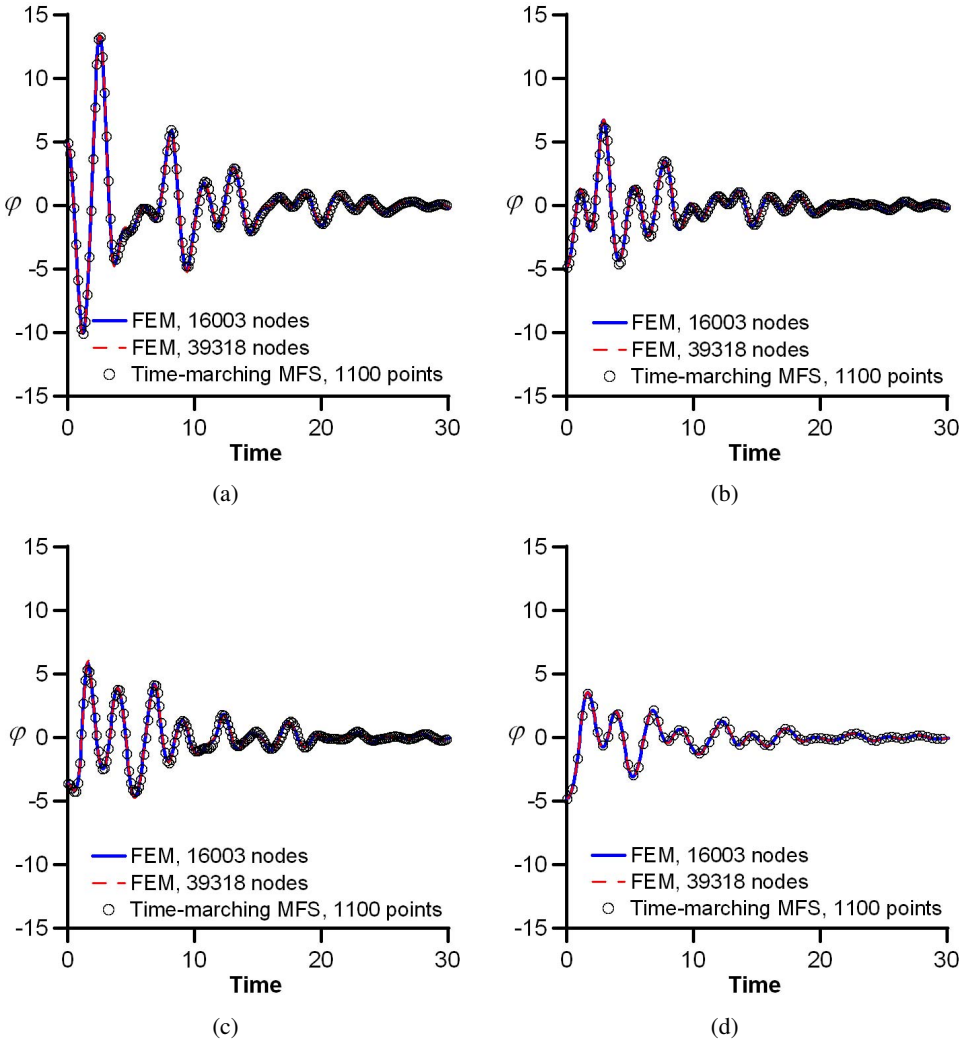


Figure 17: The evolution of φ for example 6 in slices at $(x, y, z) =$ (a)(0, 0, 0) (b)(0, 0, -1.5) (c)(0, 0, 1.5) (d)(1.5, 0, -1).

pable of obtaining similar solution as mesh-dependent numerical methods in fixed boundary problems. Since the meshless numerical methods have the above advantages, further application using present algorithm in solving telegraph equation problems can be expected for future science researches or engineering applications.

Acknowledgement: The National Science Council (NSC) of Taiwan is grate-

fully acknowledged for providing the financial support to carry out the present work under Grant No. NSC-97-2221-E-002-247-MY3 and NSC-99-2811-E-002-010. It is greatly appreciated.

References

- Amaziane, B.; Naji, A.; Ouazar, D.** (2004): Radial basis function and genetic algorithms for parameter identification to some groundwater flow problems. *CMC: Computers, Materials & Continua*, vol.1, no.2, pp. 117-128.
- Atluri, S. N.; Han, Z. D.; Shen, S.** (2003): Meshless local Petrov-Galerkin (MLPG) approaches for solving the weakly-singular traction & displacement boundary integral equations. *CMES: Computer Modeling in Engineering & Sciences*, vol. 4, no. 5, pp. 507–517.
- Chen, C. S.; Brebbia, C. A.; Power, H.** (1999): Dual reciprocity method using compactly supported radial basis functions. *Commun. Numer. Methods. Eng.*, vol. 15, no. 2 pp. 137-150.
- Cho, H. A.; Golberg, M. A.; Muleshkov, A. S.; Li, X.** (2004): Trefftz methods for time dependent partial differential equations. *CMC: Computers, Materials & Continua*, vol. 1, no. 1, pp. 1-37.
- Crespo, A. J. C.; Gómez-Gesteira, M.; Dalrymple, R. A.** (2007): Boundary conditions generated by dynamic particles in SPH methods. *CMC: Computers, Materials & Continua*, vol. 5, no. 3, pp. 173-184
- Davies, A. J.; Crann, D.; Kane, S. J.; Lai, C. H.** (2007): A hybrid Laplace transform/finite difference boundary element method for diffusion problems. *CMES: Computer Modeling in Engineering & Sciences*, vol. 18, no. 2, pp. 79-85.
- Dehghan, M.; Ghesmati, A.** (2010): Combination of meshless local weak and strong (MLWS) forms to solve the two dimensional hyperbolic telegraph equation. *Eng. Anal. Boundary Elem.*, vol. 34, no. 4, pp. 324-336.
- Dehghan, M.; Shokri, A.** (2007): A numerical method for solving the hyperbolic telegraph equation. *Numer. Meth. Part. D. E.*, vol. 24, no. 4, pp. 1080-1093.
- Divo, E.; Kassab, A. J.** (2005): Transient non-linear heat conduction solution by a dual reciprocity boundary element method with an effective Posteriori error estimator. *CMC: Computers, Materials & Continua*, vol. 2, no. 4, pp. 277-288.
- Gao, F.; Chi, C. M.** (2007): Unconditionally stable difference schemes for a one-dimensional linear hyperbolic equation. *Appl. Math. Comput.*, vol. 187, no. 2, pp. 1272-1276.
- Golberg, M. A.** (1995): The method of fundamental solutions for Poisson equations. *Eng. Anal. Boundary. Elem.*, vol. 16, no. 3, pp. 205-213.

Gu, M. H.; Young, D. L.; Fan, C. M. (2009): The method of fundamental solutions for one-dimensional wave equations. *CMC: Computers, Materials & Continua*, vol. 11, no. 3, pp. 185–208.

Han, Z. D.; Atluri, S. N. (2003): Truly meshless local Petrov-Galerkin (MLPG) solutions of traction & displacement BIEs. *CMES: Computer Modeling in Engineering & Sciences*, vol. 4, no. 6, pp. 665-678.

Houbolt, J. C. (1950): A recurrence matrix solution for the dynamic response of elastic aircraft. *J. Aeronaut. Sci.*, vol. 17, no. 9, pp. 540-550.

Kapradze, V. D.; Aleksidze, M. A. (1964): The method of functional equations for the approximate solution of certain boundary value problem. *Comput. Math. Math. Phys.*, vol. 4, no. 4, pp. 82-126.

Lin, H.; Atluri, S. N. (2001): The meshless local Petrov-Galerkin (MLPG) method for solving incompressible Navier-Stokes equations. *CMES: Computer Modeling in Engineering & Sciences*, vol. 2, no. 2, pp. 117-142.

Liu, C. S. (2010): An analytical method for computing the one-dimensional backward wave problem. *CMC: Computers, Materials & Continua*, vol. 13, no. 3, pp. 219-234.

Liu, C. S.; Chang, J. R.; Chang, K. H.; Chen, Y. W. (2008): Simultaneously estimating the time-dependent damping and stiffness coefficients with the aid of vibrational data. *CMC: Computers, Materials & Continua*, vol. 7, no. 2, pp. 97-107.

Mathon, R.; Johnson, R. L. (1977): The approximate solution of elliptic boundary-value problems by fundamental solutions. *SIAM J. Numer. Anal.*, vol. 14, no. 4, pp. 638-650.

Ortega, R.; Robles-P'erez, A. M. (1998): A maximum principle for periodic solutions of the telegraph equation. *J. Math. Anal. Appl.*, vol. 221, no. 2, pp. 625-651.

Soroushian, A.; Farjoodi, J. (2008): A unified starting procedure for the Houbolt method. *Commun. Numer. Methods. Eng.*, vol. 24, no. 1, pp. 1-13.

Sun, X. S.; Huang, L. X.; Liu, Y. H.; Cen, Z. Z. (2004): Elasto-plastic analysis of two-dimensional orthotropic bodies with the boundary element method. *CMES: Computer Modeling in Engineering & Sciences*, vol.1, no.1, pp. 91-105.

Tsai, C. C.; Young, D. L.; Cheng, A. H. D. (2002): Meshless BEM for three-dimensional Stokes flows. *CMES: Computer Modeling in Engineering & Sciences*, vol. 3, no. 1, pp. 117-128.

Wang, H.; Qin, Q. H.; Kang, Y. L. (2006): A meshless model for transient heat conduction in functionally graded materials. *Comput. Mech.*, vol. 38, no. 1, pp.

51-60.

Wen, P. H.; Chen, C. S. (2009): The method of particular solutions for solving scalar wave equations. *Commun. Numer. Meth. Engng.*, DOI: 10.1002/cnm.1278.

Young, D. L.; Chen, C. H.; Fan, C. M.; Shen, L. H. (2009): The method of fundamental solutions with eigenfunction expansion method for 3D nonhomogeneous diffusion equations. *Numer. Meth. Part. D. E.*, vol. 25, no. 1, pp. 195-211.

Young, D. L.; Chen, C. S.; Wong, T. K. (2005): Solution of Maxwell's equation using the MQ method. *CMC: Computers, Materials & Continua*, vol. 2, no.4, pp. 267-276.

Young, D. L.; Chen, K. H.; Liu, T. Y.; Shen, L. H.; Wu, C. S. (2009): Hypersingular meshless method for solving 3D potential problems with arbitrary domain. *CMES: Computer Modeling in Engineering & Sciences*, vol. 40, no. 3, pp. 225-269.

Young, D. L.; Fan, C. M.; Hu, S. P.; Atluri, S. N. (2008): The Eulerian-Lagrangian method of fundamental solutions for two-dimensional unsteady Burgers' equations. *Eng. Anal. Boundary Elem.*, vol. 32, no. 5, pp. 395-412.

Young, D. L.; Fan, C. M.; Tsai, C. C.; Chen, C. W.; Murugedsan, K. (2006): Eulerian-Lagrangian method of fundamental solutions for multi-dimensional advection-diffusion equation. *Int. J. Math. Forum*, vol. 1, pp. 687-706.

Young, D. L.; Gu, M. H.; Fan, C. M. (2009): The time-marching method of fundamental solutions for wave equations. *Eng. Anal. Boundary Elem.*, vol. 33, no. 12, pp. 1411-1425.

Young, D. L.; Tsai, C. C.; Fan, C. M. (2004): Direct approach to solve nonhomogeneous diffusion problems using fundamental solutions and dual reciprocity methods. *J. Chin. Inst. Eng.*, vol. 27, no. 4, pp. 597-609.

Young, D. L.; Tsai, C. C.; Lin, Y. C.; Chen, C. S. (2006): The method of fundamental solutions for eigenfrequencies of plate vibrations. *CMC: Computers, Materials & Continua*, vol. 4, no. 1, pp. 1-10.

Young, D. L.; Tsai, C. C.; Murugesan, K.; Fan, C. M.; Chen, C. W. (2004): Time dependent fundamental solutions for homogeneous diffusion problems. *Eng. Anal. Boundary Elem.*, vol. 28, no. 12, pp. 1463-73.